ARCHIVES OF ELECTRICAL ENGINEERING VOL. 68(3), pp. 511–520 (2019)

DOI 10.24425/aee.2019.129338

Energy efficiency analysis of railway turnout heating system with a melting snow model heated by classic and contactless heating method

MATEUSZ FLIS

Polish Naval Academy of the Heroes of Westerplatte
81-127 Gdynia, ul. Śmidowicza 69, Poland
email: m.flis@amw.gdynia.pl

(Received: 14.12.2018, revised: 04.03.2019)

Abstract: Maintaining railway turnout operability is crucial for ensuring railway transport safety. Electric heating of railway turnouts is a significant technical and economic issue. The classical heating is characterised by high power consumption. For this reason, research is needed to optimise the current system. This paper presents results of a numerical analysis and of experimental researches. The numerical analysis was carried out using the ANSYS software. There was conducted a numerical comparative analysis of energy loss during heating performed using two different heaters. Including the classical method and a heater thermally insulated from a rail. In the first step, heating of a working space filled with a substitute snow model was considered. The snow-covered surface area was held within the working space of the turnout. It was assumed that the snow substitute material had thermal properties approximately the same as real light snow. It was also assumed that the material is in the solid state which would not undergo a phase change. In the next step, a real snow model that included the phase change process was taken into account. The energy efficiency and heat distribution in the turnout have been analysed and compared. The experimental researches were carried out in a physical model. The results showed that the use of a contactless heater results in creating a larger area over which emitted heat affected snow in the working space. Consequently, more snow was melted around the contactless heater than the classic one. This experimental observation supported the results of the numerical analyses presented previously.

Key words: electrical heating, enthalpy method, experimental research, melting process, railway turnouts, thermal field, heat distribution

1. Introduction

Maintaining railway turnout operability is crucial for ensuring railway transport safety [1, 2]. Electric heating of railway turnouts is a significant technical and economic issue [3, 4]. A classic heating is characterised by high power consumption. For this reason, research is needed to optimise the power consumption [4, 5].

This paper presents results of a numerical analysis and of experimental researches. The numerical analysis was carried out using the ANSYS software. There was conducted a numerical comparative analysis of energy loss during heating performed using two different heaters. Including a classic method and a heater thermally insulated from a rail. In the first step, heating of a working space filled with a substitute snow model was considered. The snow-covered surface area was held within the working space of the turnout. It was assumed that the snow substitute material had thermal properties approximately the same as real light snow. It was also assumed that the material is in the solid state which would not undergo a phase change [5]. In the next step, a real snow model that included the phase change process was taken into account. The energy efficiency and heat distribution in the turnout has been analysed and compared.

The experimental researches were carried out in a physical model. The results showed that the use of a contactless heater results in creating a larger area over which emitted heat affected snow in the working space. Consequently, more snow was melted around the contactless heater than the classic one. This experimental observation supported the results of the numerical analyses presented previously.

2. Heating models

A model rail turnout (Figs. 1, 2) was taken for the computations. It is consisted of a stock rail, a switch rail, a classic (Fig. 1(a)) or contactless heater (Fig. 1(b)) and melting snow.

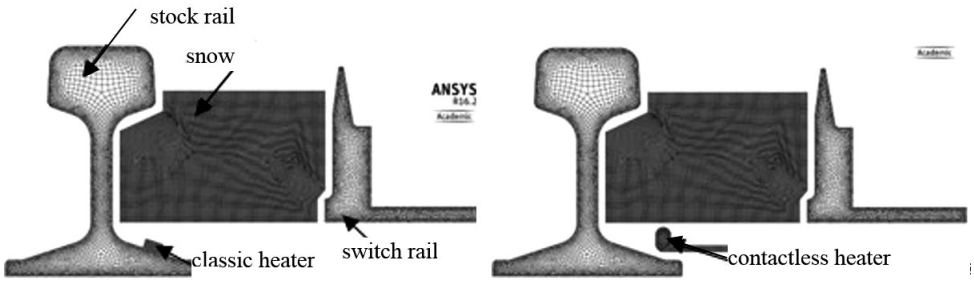

(a) (b)

Fig. 1. Models of MES created for railway turnout used in numerical simulations; Figures were showed without MES in the air area

In the railway turnout it is possible to distinguish two zones that are heated. The first zone is placed in the area under slide chairs of the turnout. The second zone is placed between the chairs. The proposed contactless heater is designed to be mounted in the second zone, whereas

the classic heater is thought to be installed in the first zone. The contactless heater is fixed directly on the rail in the first zone (there is a contact between the heater and the rail) and it is bent in a way that provides thermal insulation between the heater and the rail in the second zone. In addition to that, in the case of the contactless heater, a radiator is added to the construction of the heating element.

The actual profile of a 49E1 rail was reproduced in the model (a mass of 49 kg per meter, a height of 149 mm and the wideness of the rail's bottom side), alongside approximately real-life size heaters and a moveable rail (switch rail). The snow-covered surface area held within the working space of the switch was around 11000 mm^2 (Fig. 1, 2).

The analysed calculation area was divided into appropriate sub-areas, described with the following equations [5, 6]:

1) equation of thermal conduction describing heat transfer inside solid bodies and between the classic heater and the base of the rail

$$q_{cd} = -k\nabla T, \tag{1}$$

where q_{cd} is the heat flux density [W/m^2], k is the material's conductivity [W/(m-K)], ∇T is the temperature gradient [K/m];

2) convection heat transfer (convective heat transfer is calculated dynamically) describing heat transfer between solid bodies and fluids

$$q_{cn} = h(T_s - T_f), \tag{2}$$

where q_{cn} is the convective heat flux [W/m^2], h is the average convective heat exchange coefficient [W/(m^2-K)], T_s is the temperature of the solid [K], T_f is the temperature of the adjacent fluid [K];

3) heat transfer by radiation describing heat radiated by all bodies

$$q_r = \varepsilon\sigma T^4, \tag{3}$$

where q_r is the radiated heat flux [W/m^2], ε is the object's surface emissivity coefficient [–], σ is the Stefan-Boltzmann constant [W/(m^2-K^4)], T is the radiating object's surface temperature [K].

A mathematical model of a phase change is complicated [6, 7]. In the case that takes into account conduction, convection and the division surface between melting snow and surrounding air, it consists of [7]:

– conservation of mass

$$\frac{\partial v_x}{\partial x} + \frac{\partial v_y}{\partial y} + \frac{\partial v_z}{\partial z} = 0, \tag{4}$$

where v_x, v_y, v_z represent the velocity [m/s], x, y, z are the coordinates,

– conservation of momentum

$$\rho\frac{\partial v_x}{\partial t} + \rho v_x\frac{\partial v_x}{\partial x} + \rho v_y\frac{\partial v_x}{\partial y} + \rho v_z\frac{\partial v_x}{\partial z} = -\frac{\partial p}{\partial x} + \nabla\cdot(\mu\nabla v_x) + G_x + S_{vx} + F_{\sigma x}, \tag{5}$$

$$\rho\frac{\partial v_y}{\partial t} + \rho v_x\frac{\partial v_y}{\partial x} + \rho v_y\frac{\partial v_y}{\partial y} + \rho v_z\frac{\partial v_y}{\partial z} = -\frac{\partial p}{\partial y} + \nabla\cdot\left(\mu\nabla v_y\right) + G_y + S_{vy} + F_{\sigma y}, \tag{6}$$

$$\rho\frac{\partial v_z}{\partial t}+\rho v_x\frac{\partial v_z}{\partial x}+\rho v_y\frac{\partial v_z}{\partial y}+\rho v_z\frac{\partial v_z}{\partial z}=-\frac{\partial p}{\partial z}+\nabla\cdot(\mu\nabla v_z)+G_z+S_{vz}+F_{\sigma z}\,, \tag{7}$$

where ρ is the density [kg/m^3], t is the time [s], p is the pressure [N/m^2], μ is the viscosity [kg/s], G, S_v, F_σ are the sources [kg/m^2-s^2],

– conservation of energy in enthalpy method

$$\frac{\partial}{\partial t}(\rho H)+\nabla\cdot(\rho v H)=\nabla\cdot(\lambda\nabla T)+S_T\,, \tag{8}$$

where H is the enthalpy [J/kg], T_0 is the reference temperature [K], T is the temperature [K], β is the volume fraction [-], h_{ref} is the reference enthalpy [J/kg].

Enthalpy H is calculated as follows:

$$H(T)=h_{\text{ref}}+\beta Q_L+\int_{T_0}^{T}c_p\,\mathrm{d}T. \tag{9}$$

The volume of fraction β is calculated as:

$$\beta=\begin{cases}0 & T<T_s\\ \dfrac{T-T_s}{T_l-T_s} & \text{for}\quad T_s<T<T_l\\ 1 & T>T_l\end{cases}, \tag{10}$$

whereas source S is calculated for each direction as:

$$S_{vx}=C\frac{(1-\beta)^2}{\beta^3+\varepsilon_0}v_x\,, \tag{11}$$

where C is the mushy zone constant, ε_0 is a little number preventing from diving by zero.

3. Snow melting process

In this step a heat transfer in the model filled with real light snow was considered. In this case the snow's model undergoes a phase change and the melted liquid is falling down onto the heater's radiator and rail's foot. It was assumed that the snow has properties of real fluffy and light snow. In addition, the melting point temperature of the snow $T_l = 273.5$ K, the solidification point temperature of the snow $T_s = 272.5$ K and latent heat of phase transition $Q_L = 335$ kJ/kg. It was also assumed that the air reference temperature $T_0 = 272$ K.

In this case an extremely short geometric step was needed, also an extremely low time step, in order to maintain iterative numerical computation convergence [6, 7]. The results showed in this paragraph took about 6 months of computation on PC: 3.5 GHz, 8 cores, 128 GB RAM. It would be possible to get full melting process by means of a suitable computer system and available license. Licenses varies from each other by the number of cores that can be used, which is related to the cost of such software.

Because of melting snow flow, another continuous equation [7] was computed:

$$\frac{\partial \alpha_l}{\partial t} + u_x \frac{\partial \alpha_l}{\partial x} + u_y \frac{\partial \alpha_l}{\partial y} + u_z \frac{\partial \alpha_l}{\partial z} = 0, \tag{12}$$

where α_l is the volume fraction of liquid in the finite element [–], α_s is the volume fraction of solid in the finite element [–], u is the velocity [m/s].

Moreover, the following equation is satisfied [7]:

$$\alpha_l + \alpha_s = 1. \tag{13}$$

The results of heat distribution analysis at the end of the computation time (t = 240 s) are shown in Fig. 2. The temperatures obtained from the analysis with an activated modulus of melting and snow flow are shown in Fig. 2(a), Fig. 2(b). The classic heater's temperature arises up to 297 K, whereas it is as high as 339 K in the contactless case. The results show that the temperature of the contactless heater is higher that the temperature in the classic one.

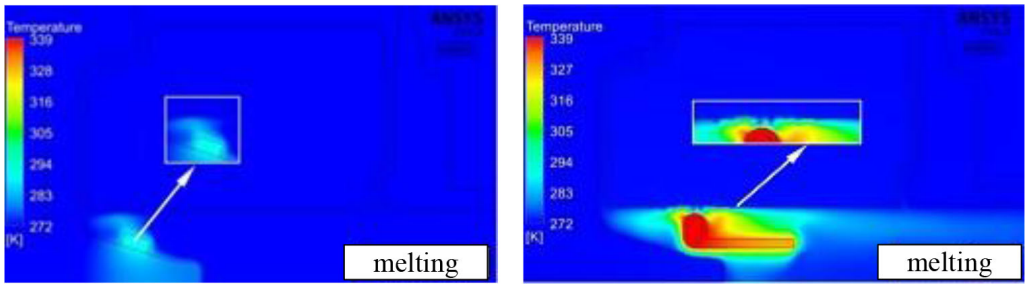

(a) (b)

Fig. 2. Temperature field distribution in model: (a) classic with melting; (b) contactless with melting, for time t = 240 s

A volume fraction distribution in the case is shown in Fig. 3. It can be seen that in the case of the contactless heater the snow starts to melt after 200 s. The process is propagating and when the time reaches t = 240 s there are significant differences between both heating systems. In the system heated in a classic way the snow didn't start to melt as opposed to the second heating system. It's important to say that the melted snow, which lays on the heater radiator, is a subject to evaporation. The part of the melted snow that lays on the rail foot, freezes again, because of the rail foot temperature with is well below the solidus temperature.

Beside those distributions, an arbitrarily chosen temperature distribution at time t = 240 s is also presented (Fig. 4). It is showed that about 30% of the snow zone gets temperature equal or higher than 272.5 K, when the railroad turnout is heated by the newly proposed contactless heater (Fig. 4(b)). It is only about 10% when it is heated in a classic way (Fig. 4(a)).

Fig. 5 shows a chart of temperature T in a function of time for the model with a melting process in the classic system (T_{kp}) and contactless system (T_{bp}). The temperature charts were obtained for points, where the temperature was the highest.

The points are showed in Fig. 5. The process of absorption of latent heat Q_L is clearly seen on both charts. It is shown that in the case of the classic heater the melting process takes much more

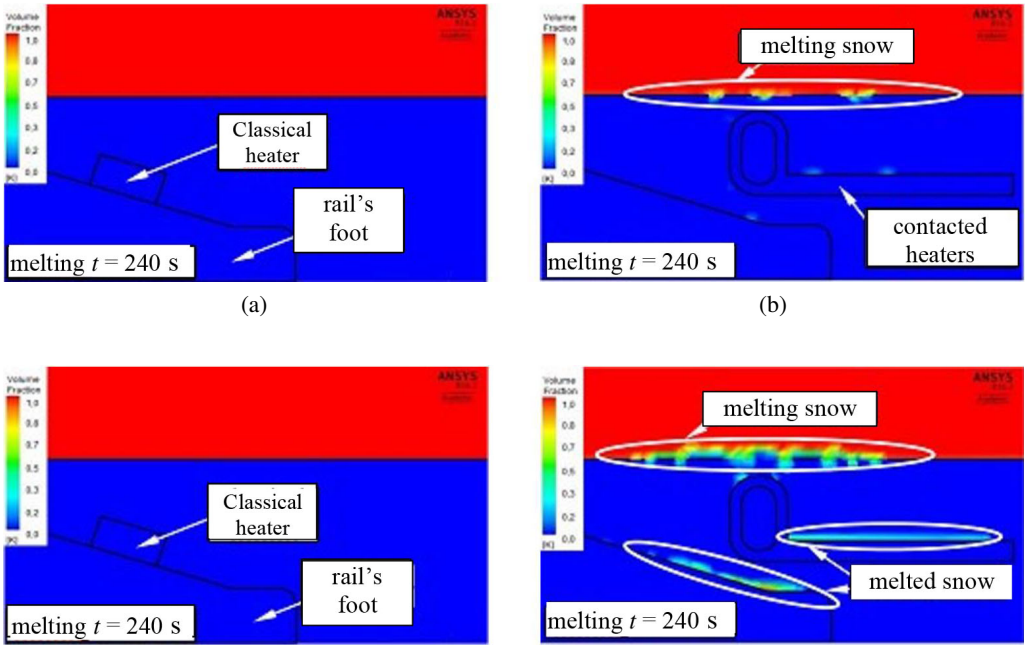

Fig. 3. Volume fraction distribution in the models: (a) classic for t = 200 s; (b) contactless for t = 200 s; (c) classic for t = 240 s, (d) contactless for t = 240 s

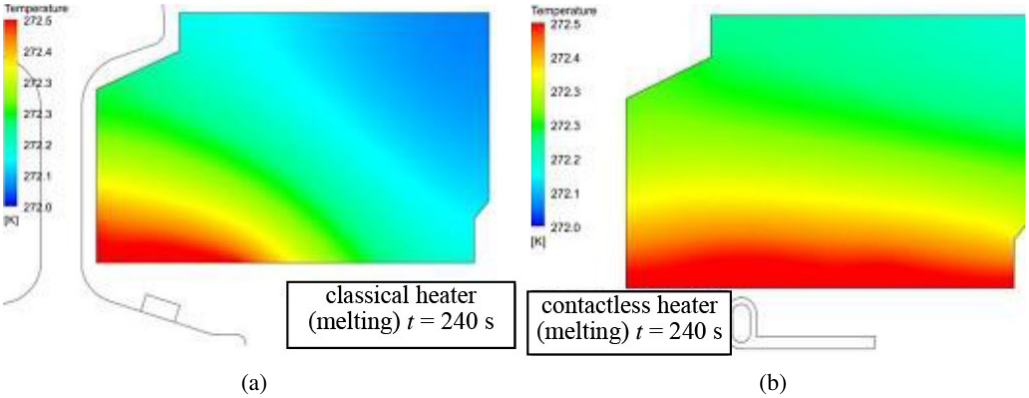

Fig. 4. Heat distribution in the snow zone in the model: (a) classic with melting; (b) contactless with melting; the distributions are showed for the time t = 240 s, for the area $T \leq 272.5$ K red colour is used

time in contrast to the contactless heater system, where the melting starts after 39 s of heating and lasts for 186 s. In the classic solution the time needed to start melting is twice as high as in the contactless heater.

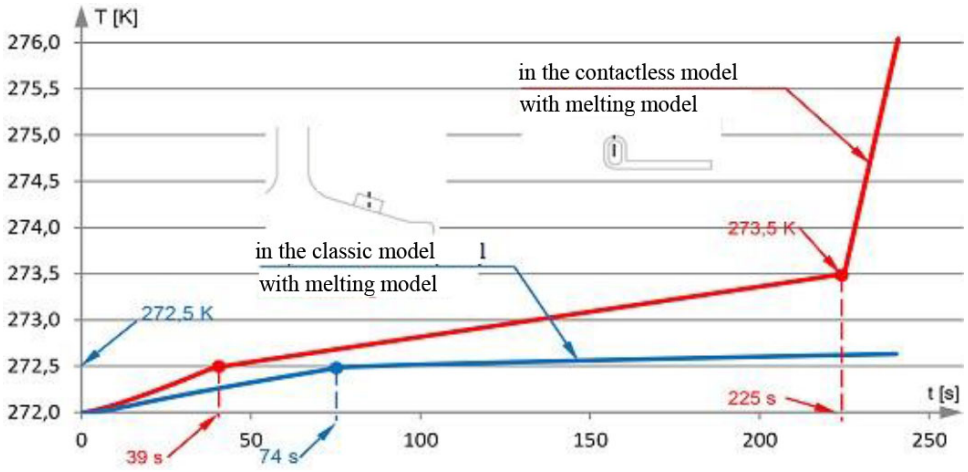

Fig. 5. Temperature (T) chart in a function of time for the model with melting process: classic heater (T_{kp}), contactless heater (T_{bp})

4. Experimental research on snow melting process

The experimental research was carried out in a physical model. The model consists of a stock rail, moveable rail and a contactless heater (Fig. 6) or a classic heater (Fig. 7).

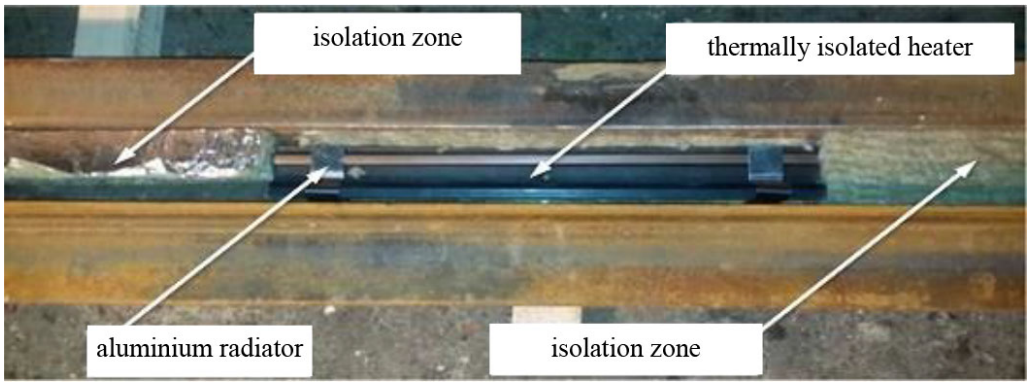

Fig. 6. Zone heated in a contactless way

A Flir B60 thermal camera was used to measure temperatures of the heaters and rail's head. This experimental observation supports (Figs. 8, 9) the results of the numerical analyses presented previously. The results are shown in the pictures.

The experimental measurements were taken at a sub-zero temperature, after the physical model had been covered in snow (Fig. 10). The heating was terminated after 90 minutes of continuous heating. Fig. 10 shows how much snow had melted in that time. Thus, the use of

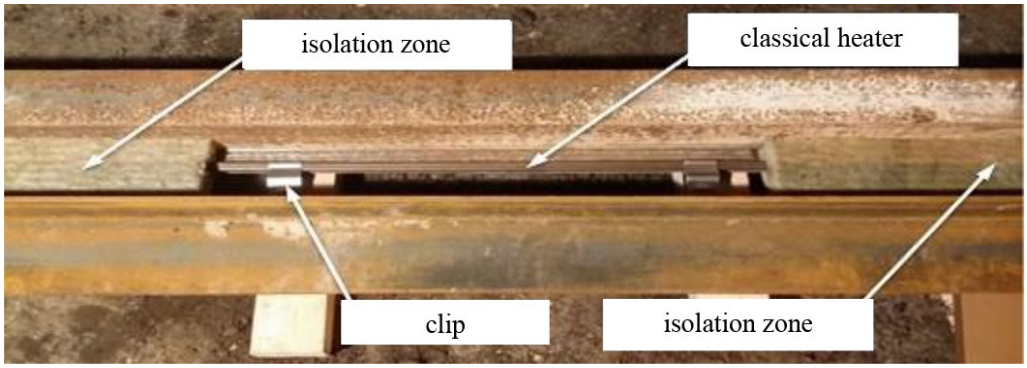

Fig. 7. Zone heated in a classic way

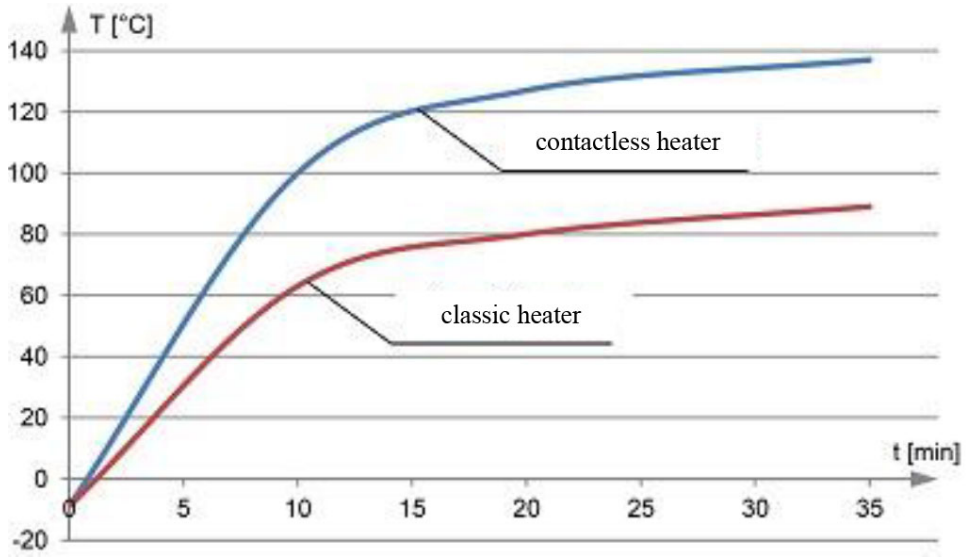

Fig. 8. Results of heater's temperature measurement for: classic heater, contactless heater

a contactless heater results in creating a larger area over which emitted heat affects snow in the working space of the turnout. Consequently, more snow is melted around the contactless heater than around the classic one.

Both showed numerical experiments present that a railroad turnout heated by a contactless heater is characterised with higher efficiency than its classic counterpart. The railroad working area is free of snow faster and thus it consumes less energy. The newly proposed solution favours a more ecological approach, which is extremely important nowadays. The futher research is needed to optimise calculation time. It is reasonable to look for less complex and efficient software that can solve the stated problem in less time. It would probably be an authorship program dedicated for this specific application.

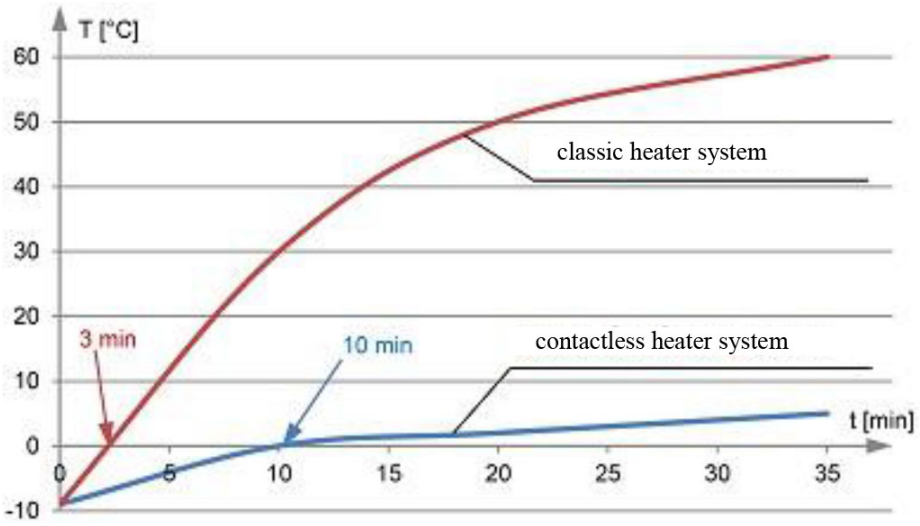

Fig. 9. Results of stock's rail temperature measurement for: classic heater system, contactless heater

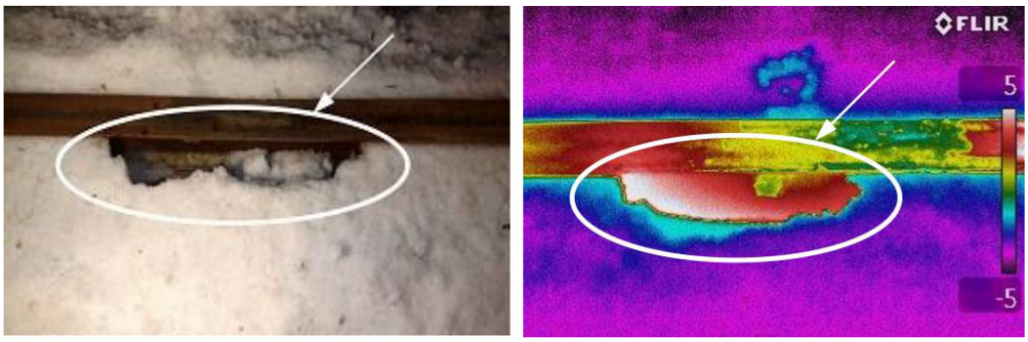

(a) (b)

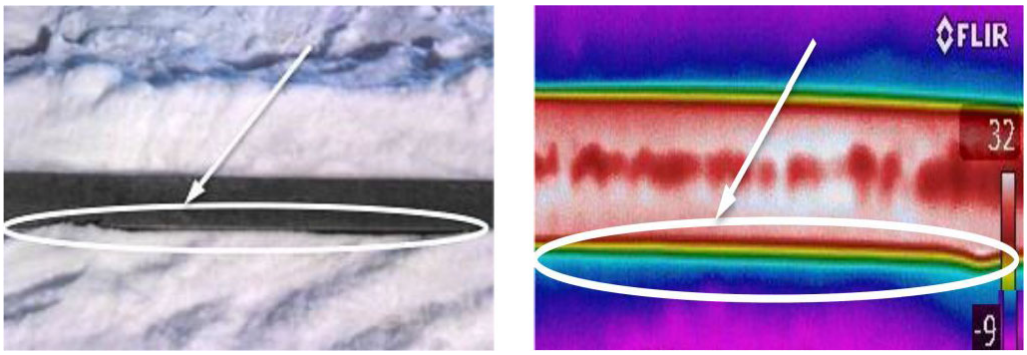

(c) (d)

Fig. 10. Zones after 90 minutes of heating with contactless heater: (a) photo; (b) termograph, with classic heater; (c) photo; (d) thermograph [5]

5. Conclusions

The comparative analysis of energy loss during heating of two models of a railway turnout showed considerable energy consumption while heating a railway turnout in a traditional way. Heating the area close to a fixed rail (stock rail) and a moveable rail (switch rail) requires a relatively large amount of electric energy. Using a contactless heater facilitates heating the area close to the rail while incurring a small energy loss.

In the presented case, a temperature of 272.5 K on the border of the snow zone (Fig. 5) appears twice faster using the contactless heater system than in a classic heater system. The experimental results, where the temperature of melting is slightly higher, namely 273 K, show that the time needed for the start of the melting process is three times shorter when using the contactless heater, thus the electrical energy consumption of the contactless heater is smaller.

References

[1] Flis M., *An overview over the methods of snow melting in railway turnouts*, Electrical Engineering, Poznan University of Technology Academic Journals (in Polish), Poznań, no. 83 (2015).

[2] Brodowski D., Andrulonis J., *Railway turnouts heating*, Railway Issues (in Polish), Warsaw, no. 135 (2002).

[3] Wołoszyn M., Jakubiuk K., Flis M., *Analysis of resistive and inductive heating of railway turnouts*, Przegląd Elektrotechniczny, no. 4 (2016).

[4] Brodowski D., *Railway turnouts heating – the new method. Contactless heating as a way to melt snow in the turnout faster*, Technical information, Railway Institute (in Polish), Warsaw (2012).

[5] Flis M., Wołoszyn M., *Energy Efficiency Analysis of Railway Turnout Heating with a Simplified Snow Model Using Classical and Contactless Heating Method*, International Interdisciplinary PhD Workshop, 8th International Interdisciplinary PhD Workshop Conference, The Conference Proceedings, IEEE Xplore Database [ISSN: 1897-0737] (2018).

[6] Wiśniewski S., Wiśniewski T., *The heat transfer*, no. 4, WNT (in Polish), Warsaw, ISBN 83-204-2110-1, no. 4 (1997).

[7] *ANSYS Fluent Theory Guide, Release 15.0*, ANSYS Inc., November (2013).